Birefringence Free Planar Optical Waveguide Made by Flame Hydrolysis Deposition (FHD) Through Tailoring of the Overcladding

A. Kilian, J. Kirchhof, B. Kuhlow, G. Przyrembel, and W. Wischmann

***Abstract*—Stresses developing in a planar waveguide resulting from the different thermal expansion coefficients of the substrate and the three glass layers (buffer, core and cladding) were analyzed using a finite element method. It can be shown that mainly the thermal expansion of the overcladding determines the birefringence in the finished waveguide. Based on that result, recipes for an overcladding made with the flame-hydrolysis-deposition-(FHD)-process were devised. We demonstrate the absence of birefringence in a commercial waveguide layer overclad with this glass. The high doping levels required for the cladding to have a thermal expansion coefficient sufficient for this raises concerns about the moisture sensitivity of such a glass. We examined the depth dependent composition of the glass using WD-ESCA (wavelength dispersive electron microprobe) and show, that at the surface a layer depleted of dopants is formed during the high temperature sintering process. This layer can serve as a protective coating to isolate the underlying, higher doped layer from the effects of moisture. Analysis of the stresses shows that this does not effect the birefringence behavior of the waveguide.**

***Index Terms*—Arrayed waveguide grating, birefrigence, flame hydrolysis deposition (FHD), planar optical waveguides.**

I. Introduction

While planar optical waveguides in silica have shown enormous promise for wavelength routing application [1], [2], a problem remains with their birefringence. It is thought to result from the use of a silicon substrate, which upon cooling after the sintering or annealing of the glass layer strains the glass layer because its different expansion coefficient. The use of a silica substrate reduces this problem [3], it nevertheless is still to large for practical application. Other means of reducing the birefringence have been proposed, for example the use of high expansion glass for the waveguide layers [3], a birefringence modifying patch [4] or ultraviolet (UV)-treatment [5] of the finished waveguides. Alternatively, the effects of the birefringence can be removed by the insertion of a halfwave-plate in the middle of the filter structure [6] or stress relief grooves in close proximity to the waveguides [7].

Recently, it was shown that the layer used for covering the patterned core ribs (the overcladding) mainly influences the birefringence of the waveguide. By using the plasma chemical vapor deposition (PCVD) process to fabricate an overcladding with a suitable expansion coefficient, birefringence free waveguides were obtained [8].

In this paper, we present result obtained using flame hydrolysis deposition (FHD) for overcladding waveguide ribs. Using the finite element method, we have examined stresses resulting from different thermal expansion coefficient of the three glass layers (buffer, core, and overcladding) and the substrate in a number of planar waveguide configurations. Based on the results we have devised recipes for an overcladding made with the FHD-process and demonstrate the absence of birefringence in a waveguide layers overcladded with this glass. Our results demonstrate the surprising fact that mainly the thermal expansion of the overcladding determines the birefringence behavior of the finished waveguide. From this, it follows that it is not necessary to increase the level of dopants in the core or buffer layer to match the thermal expansion coefficient of all layers to the substrate. This would result in a reduction of softening point of the core glass and may lead to deformation of the waveguide ridges, which in turn leads to a deterioration of the filtering properties of the arrayed waveguide grating (AWG)-components [3].

SiO_2 must be doped with a very substantial amount of boron (and eventually another dopant for the adjustment of the refractive index) to have a sufficiently high thermal expansion for birefringence compensation and one has to concern oneself about the moisture sensitivity of such a glass [9]. In fact, we have made layers using FHD which after sintering were clear and turned cloudy even after a couple of hours in ambient air, nevertheless, in those cases the level of dopant was higher than required for birefringence compensation.

We have analyzed the depth dependant composition of an FHD made overcladding demonstrating that at the surface of the cladding a SiO_2-rich layer is formed due to out-diffusion of the volatile dopants at the high sintering temperature. This layer can serve as a protective coating to isolate the underlying, higher doped layer from the effects of moisture. In going back to the calculation of the stresses we show that this does not effect the birefringence behavior of the waveguide.

II. Experimental

A. Deposition and Sintering

A standard three-ring torch, which was fed with O_2 in the outer ring, H_2 and He in the middle ring and the chlorides of silicon, phosphorus and boron in the innermost tube was used

Manuscript received March 20, 1999; revised November 1, 1999. This work was supported in part by the Thüringen Ministry for Science and Technology.

A. Kilian and J. Kirchhof are with the Institut für Physikalische Hochtechnologie e.V., Jena 07745, Germany.

B. Kuhlow and G. Przyrembel are with the Heinrich Hertz Institut, Berlin, Germany.

W. Wischmann is with Alcatel Corporate Research Center, Stuttgart, Germany.

Publisher Item Identifier S 0733-8724(00)01312-8.

to generate particles and deposit onto a wafer. It is mounted pointing downward at an angle of 70°. A larger size glass tube mounted approx. 6 cm in front of the torch serves as an exhaust for the HCl formed in the flame from the hydrolysis of the chlorides. The wafer is held on a heated (200 °C) deposition platform which is moved through the flame with an XY-table. The flow rates of H_2, He, and O_2 are adjusted to give a relatively low flame temperature (compared with what is used for the deposition of the buffer and core layers). This was found to enhance the incorporation of boron and phosphorous into the layer and avoid the formation of cracks. We use $SiCl_4$, PCl_3 and BCl_3 as sources for the oxides, the former two are evaporated by bubbling helium through them, while the BCl_3 is a gas and metered directly using a mass flow controller. The flowrates of the chlorides together with other deposition parameters are adjusted to give a final glass film thickness of approximately 25 μm.

The glass-soot has a low density after deposition, upon transfer into the oven and sintering at 1100 °C in a helium atmosphere a clear glass layer forms. Typically, a 2–h ramp to 1100 °C where the temperature is held for another 2 h is used as a sintering routine. A sintering-atmosphere of pure helium was found to be important to avoid the inclusion of bubbles. Without sintering in pure helium these bubbles tend to form particularly at points where waveguide ridges slowly diverge, e.g., the entrance and exit region of a coupler.

B. Compositional Analysis

Layers were cut into several pieces, partially masked with a suitable polymer and etched in diluted HF (6%) for varying amounts of time. After removal of the polymer the etch depth was determined using a profilometer (DECTAC). Typically, the layers appeared cloudy after prolonged etching, which is commonly observed even when etching pure silica and does not necessarily indicate phase separation in the glass layer. However, this results in surface roughness, which increases the error of the compositional analysis and should be taken into account when looking at the measurements at an etch depth larger than 10 μm.

The analysis was performed using a JEOL JXM 8800S superprobe instrument. As a standard for calibration we used B-metal, SiO_2 and GaP and NaCl (we also probed for residual chlorine, but did not find any in the samples). The measured values were corrected using the ZAF-correction procedure of the instrument software. Judging from previous experience, the boron- and silicon-content given is precise to ± 1 weight%, while the phosphorus can be measured precisely to ± 0 5 weight%. One has to keep in mind that an EDAX measurement gives the average composition over a certain depth, which in the case of this light elements can be assumed to be between 1 to 2 μm. Because of this the first measurement does not give the real values at the surface, which can be assumed to consist almost of pure SiO_2 because of the volatility of the boron- and phosphorous-oxides.

Shown in Fig. 1 are etch time and analyzed composition of a sample deposited under similar conditions as sample #1.

C. Thermal Expansion Measurements

The thermal expansion coefficient of the layers was determined by measuring the curvature of a 0.5-mm wafer with an FHD-layer on one side as a function of temperature on a Tencor FLX-2320 thin film stress analyzer, which determines the curvature by measuring the deflection of a laser beam scanned across the wafer. We measured every 50 °C up to 400 °C. We found that the high-temperature oxidation necessary before the deposition of the FHD-layer already resulted in bowed or even wavy wafers, so that one could not judge from their radius of curvature on the magnitude of the thermal expansion coefficient of a deposited layer. Rather, we used the fact that the thermal expansion of silicon increases from $2.3 \cdot 10^{-6}$ K^{-1} at room temperature to $3.6 \cdot 10^{-6}$ K^{-1} at temperature above 400°C [10], while at the same time the thermal expansion of B- and P-doped SiO_2 remains constant in this interval. Because of this, if the glass layer has a thermal expansion coefficient in the range from $2.3 \cdot 10^{-6}$ K^{-1} to $3.6 \cdot 10^{-6}$ K^{-1}, the wafer bow will initially increase with temperature, while at some higher temperature this reverses and the bow decreases with temperature. The thermal expansion coefficient of silicon at the temperature at which the bow reverses its direction can be assumed to be the one of the layer. To demonstrate this, in Fig. 2 we show radii of curvature as a function of temperature for two samples together with a value for the thermal expansion coefficient extrapolated from the data in [10].

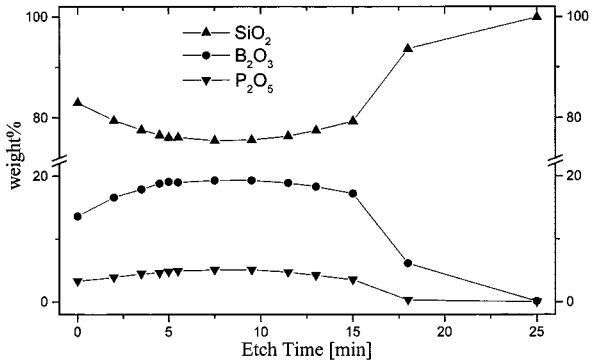

Fig. 1. Depth dependent composition of sample #1, last measurement on Si-substrate (last 2 μm are thermal oxide buffer layer).

D. Optical Measurements

In order to measure the stress-induced birefringence of the waveguides, an arrayed waveguide grating (AWG) was used because of the high sensitivity of this structure to birefringence. The AWG structure was etched into the FHD deposited core layer of a silica wafer delivered by PIRI Corporation, which in turn was overcladded with FHD silica layer. The AWG used for testing is an eight-channel 200-GHz demultiplexer for 1.55 μm center wavelength with a path length difference in the waveguide grating of $\Delta L = 126.3$ μm working in grating order $m = 118$. The center wavelength of an AWG is shifted with $\Delta\lambda$ in the transverse electric (TE) and transverse magnetic (TM) modes by waveguide birefringence B according to $\Delta\lambda = (B \cdot \Delta L)$ /m, where $B = n_{\mathrm{TM}} - n_{\mathrm{TE}}$ is the effective refractive index difference in the embedded grating waveguides for TE and TM modes. For silica-on-silicon substrate processed with standard layers as commercially available from PIRI we measured a value $\Delta\lambda = 0.26$ nm. For silica on quartz glass substrate from the same source a value $\Delta\lambda = -0.18$ nm at 1.55 μm wavelength is obtained. This corresponds to uncompensated FHD

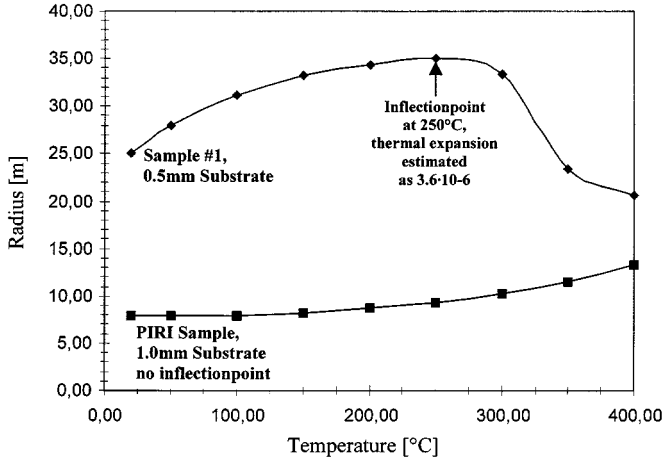

Fig. 2. Estimation of thermal expansion of the layer by measurement of the temperature dependence of its curvature.

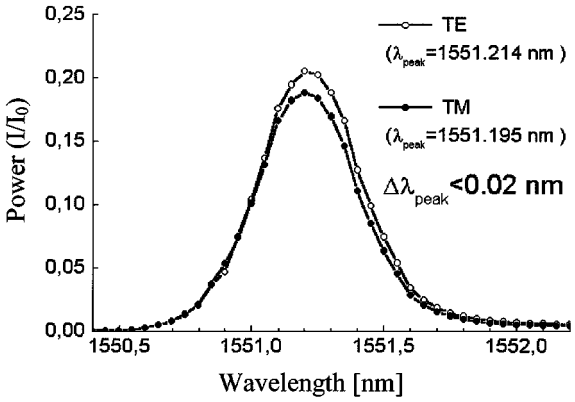

Fig. 3. Transmission wavelength spectrum for one channel of the AWG.

TABLE I

Sample number	(BCl_3 + PCl_3) -flowrate*, [arbitrary units]	Inflectionpoint of wafer bow at °C	Estimated thermal expansion [K^{-1}]	Average measured TM/TE-shift [nm]
2	1.2	230	$3{,}5\cdot10^{-6}$	-0,02
3	1.1	180	$3.3\cdot10^{-6}$	-0,02/-0,06**
4	1	140	$3.1\cdot10^{-6}$	+0.05

* The B_2O_3 and P_2O_5 ratio is adjusted to give the proper refractive index
** The second value was obtained on a sample with smaller, higher index cores

layers core birefringence $B = 2.4 \cdot 10^{-4}$ and $B = -1.7 \cdot 10^{-4}$, respectively. Fig. 3 shows the AWG transmission wavelength spectrum for one channel of a probe with reduced birefringence (in linear transmission scale for better discrimination of both polarization modes).

Here a value of $\Delta\lambda < 0.02$ nm is obtained resulting in a reduced birefringence $B < 1.8 \cdot 10^{-5}$. A remarkable change in insertion loss was not observed with this stress compensating overcladding layer. The polarization dependence of the AWG was measured using a polarization controller (Hewlett Packard HP8169A) fed from a tunable laser source (Hewlett Packard HP8168). The polarization controlled light was launched into the device input waveguide and the two polarization states with lowest and highest filter peak wavelength were determined. It reveals that these extreme polarization states with maximum $\Delta\lambda$ correspond to TE and TM polarization at the device input. We also have made additional planar waveguides, where the entire layer system (cladding, core and buffer) was deposited using our own process. Although it is highly unlikely that our core and buffer layers have a thermal expansion coefficient similar to the one of the layers made by PIRI, we obtained nearly birefringence free waveguides by overcladding either of them with a very similar cladding composition. Additionally, we have recently overcladded AWG's provided by Alcatel Corporate Research Center, Stuttgart with the results shown in Table I.

III. Modeling

For the calculation of the stresses in the core structure, it was assumed that down to a temperature at which the cladding glass solidifies the core structure is free of strain significant for the birefringence, since only stresses along the core, parallel to the propagation direction can exist while the core is free on its sides and top. The solidification temperature was assumed to be 1000 °C in all calculations, which might be somewhat high for the highly doped glasses used for the cladding, but the influence of this parameter is small. Furthermore, as will be seen, the most important requirement for the avoidance of birefringence is to match the two main stresses perpendicular to the core (that is, the stress perpendicular and parallel to the wafer surface). A different solidification temperature will affect all the layers, causing mostly a change of the magnitude of the stresses, while their difference remains constant.

The program used for the stress analysis (Antras) does not allow for a vectorial treatment of a stress problem, which could cause an error because the material parameters the single crystal silicon substrate depend on the direction. In order to minimize such errors, most of the calculations were performed using the values [11] of 169 GPa for Young's modulus and 0.064 for Poisson's ratio for the [010] direction and then checked with the values for the [011] direction, which are 130 GPa and 0.279, respectively. In none of the calculation stresses differed more than 1% for the two directions. In the calculation an average thermal expansion coefficient for silicon was used, $3.6 \cdot 10^{-6}$ K^{-1} was calculated between 273 K and 1273 K from values in [10].

The changes in refractive index for triaxial stresses in a Cartesian coordinate systems are

$$\Delta n_x = n_x - n = -B_2\sigma_x - B_1(\sigma_y + \sigma_z)$$
$$\Delta n_y = n_y - n = -B_2\sigma_y - B_1(\sigma_x + \sigma_z)$$

and

$$\Delta n_z = n_z - n = -B_2\sigma_z - B_1(\sigma_x + \sigma_y)$$

where the stress optical coefficients (for pure SiO_2-glass) are $B_1 = 4.2 \cdot 10^{-6}$ MPa^{-1} and $B_2 = 6\,5 \cdot 10^{-7}$ MPa^{-1} after [12].

Taking the y-direction as the propagation direction and z as the direction perpendicular to the wafer, it follows for the stress-induced birefringence:

$$\Delta n_x - \Delta n_z = -(B_2 - B_1)(\sigma_x - \sigma_z).$$

In order to calculate the waveguide birefringence properly, one would have to use the refractive index distribution resulting

TABLE II

Substrate	*SiO_2*	*Si 100**																		
	No Diffusion (homogeneous cladding)															Diffusion**			Coupler***		
Thick.$_{Sub}$ [mm]	1	1								0,5			1			1			1		
Thick.$_{clad}$ [μm]	30	30								30			20			30			30		
α_{buffer} ($\cdot 10^6$)	0.8	1.2	1.8	1.2			1.2		1.8	1.2			1.2			1.2			1.2		
α_{core} ($\cdot 10^6$)	1.0	1.8	1.8	1.8			2.4		2.4	1.8			1.8			1.8			1.8		
α_{clad} ($\cdot 10^6$)	1.2	2.4	2.4	3.4	3.45	3.5	3.45	3.5	3.45	3.3	3.4	3.45	3.4	3.45	3.5	3.4	3.45	3.5	3.4	3.45	3.5
σ_{xx} [N/mm^2]	20.33	-105.4	-109.4	-73.4	-71.8	-70.1	-45.8	-44.2	-48.6	-72.49	-70.43	-68.83	-74.47	-72.15	-70.34	-73.4	-71.8	-70.1	-49.63	-48.13	-46.63
σ_{yy} [N/mm^2]	10.6	-130.9	-135.6	-142.4	-142.4	-141.9	-89.5	-90.0	-93.0	-139.9	-140.4	-140.9	-144.5	-144.7	-145	-142.4	-142.4	-141.9	-137.2	-137.6	-138.0
σ_{zz} [N/mm^2]	-8.99	-26.16	-26.16	-69.4	-71.57	-73.73	-45.5	-47.66	-45.54	-68.92	-71.65	-73.72	-67.61	-70.26	-72.37	-69.4	-71.57	-73.73	-65.44	-67.47	-69.47
Δn ($\cdot 10^5$)	10.4	-28.1	-29.6	-1.43	-0.064	1.29	-0.106	1.25	-1.08	-1.27	0.43	1.74	-2.44	-0.67	0.72	-1.43	-0.064	1.29	5.61	6.87	8.11

* $\alpha_{\mathrm{substrate}}$ taken as $3.6 \cdot 10^{-6}$ (average value between 20° and 1000 °C calculated from [10]). All calculations were performed for the 100 and 110 direction of the silicon substrate. While σ_{zz} is barely influenced by the direction, σ_{xx} and σ_{yy} are on average 0.8 N/nm^2 lower in the 110 direction, resulting in a Δn which is on average $0.2 \cdot 10^{-5}$ higher.

** Upper 5 μm of cladding are assumed to have α of $0.9 \cdot 10^{-6}$ to examine the influence of out-diffusion of dopants.

*** Evanescent Field Coupler: two 6 by 6 μm core ridges spaced 6 μm apart homogeneous cladding.

from the stresses to calculate the difference in the propagation constant for the two polarization directions of the light. This rather complicated procedure was avoided by estimating the birefringence from the average of the refractive index difference $\Delta n_x - \Delta n_z$ in the center region of the core. In Fig. 4, we plot an example of a stress distribution across the centerline of the core in x and z direction. In the central region of the core, where most of the light is guided, the stresses are fairly constant.

This gives us confidence that the simplification causes a tolerably small error. However, in some instances, particularly when a smaller core with a slightly higher index had been overcladded (see Table I), the birefringence was measured to increase. Apparently, in this case, the different distribution of energy in the guided mode led to more light being guided in regions where the respective indices are less well matched. We believe that in those cases a readjustment of the thermal expansion coefficient of the cladding again will lead to a birefringence free waveguide.

For the calculations a standard geometry was chosen as a 6 by 6-μm core on a 20-μm thick buffer layer. The E-module of the buffer glass was taken as 72 500 N/mm^2, which is the value for pure quartz glass, while 65 000 N/mm^2 was used for the cladding glass, the value for Pyrex, which has a similar dopant level, also primarily boron, as the cladding. 70 000 N/mm^2 was taken for the core as an intermediate level. Similarly, 0.17, 0.2, and 0.2 were used for Poison's constant, for the buffer, core and cladding, respectively.

Parameters varied included the thickness of the substrate and the cladding, and the thermal expansion coefficient of the buffer, core, and cladding glass composition. Other configurations examined included a thick cladding layer, where the top 5 μm had a reduced thermal expansion coefficient to model the influence of the out-diffusion of a volatile dopant during the sintering process and a coupler geometry with two 6 by 6 μm cores separated by a 4-μm spacing.

IV. Discussion

Results of the calculations are presented in Table II. In the first column we show results for a quartz glass substrate with a thermal expansion coefficient α of $0.8 \cdot 10^{-6}$ K^{-1} (for the core we estimated α of $1.0 \cdot 10^{-6}$ K^{-1} because at least some germanium doping is needed to increase the refractive index, while the cladding is expected to have an even higher α of $1.2 \cdot 10^{-6}$ K^{-1}, since the lower sintering temperature for this layer requires doping with boron/phosphorus). As predicted by the calculation, the birefringence was measured to be smaller, but has a different sign. In the second and third column we demonstrate that with a reasonable choice of the thermal expansion coefficients our model yields values for the birefringence similar to those measured in a commercially available device (PIRI).

As can be seen in Table II, the thermal expansion coefficient of the buffer and core glass does not influence the birefringence to a significant extent. This result seems surprising, but when looking at the stresses in Fig. 4 it can be explained. In x-direction (in plane) one finds the expected compressive stress resulting from the higher thermal expansion of the substrate. But there is also significant stress in the z-direction because of the higher thermal expansion of the cladding glass compared to the core glass, which compresses the core glass in z-direction. At some point the stresses in z-direction and x-direction equal each

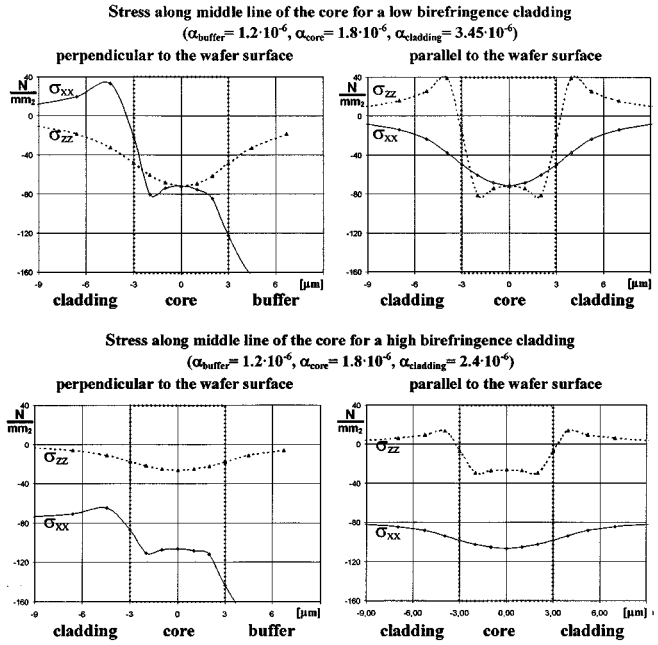

Fig. 4. Stress distribution across the centerline of the core in x and z direction.

other, resulting in very low birefringence. From the calculation follows that the glass composition of the cladding has to be tuned to give a slightly lower thermal expansion than the silicon substrate. Judging from the numbers the birefringence appears to be very sensitive to the exact match (observe the changes resulting from a variation of α_{cladding} between $3.4 \cdot 10^{-6}$ to $3.5 \cdot 10^{-6}$), but a birefringence of 10^{-5} will constitute only 1.3% $((10^{-5}/1.45) \cdot (1550\,\text{nm}/0.8\,\text{nm}))$ of a 100 GHz channel of a WDM-multiplexer, so it can be easily tolerated. The same must be said about a coupler region where two ridges of (lower expansion) core glass are close to each other. This alters the stress distribution, so that for a choice of thermal expansion coefficient giving very small birefringence in a single ridge, here some birefringence remains. So it appears that on a WDM-filter, where one finds waveguide ridges at all sorts of distances from each other, one could never completely avoid birefringence, but easily reduce it to a very low level by the proper choice of the thermal expansion coefficient of the cladding glass. While we also examined the stress distribution for a thinner substrate (0.5 mm instead of 1.0 mm) and a thinner cladding (20 μm instead of 30 μm), the results were very similar: While the magnitude of the stresses changed, the match between stresses in the x- and z-direction resulted in a birefringence free waveguide. Since it was not necessary to dope the core or buffer layers differently for this result, we believe that any deformation of the cores [4] is avoided, we did not measure a deterioration of the filtering properties of the AWG-components.

One of our concerns was that the high boron content of the glass would render it susceptible to the attack of moisture. Here, the volatility of this dopant at the high temperature at the end of the sintering procedure comes to help: the measurement of the distribution of the boron shows that at the surface a layer depleted in boron forms, which can serve as a protective coat.

No degradation was observed in samples, which had been cut with a water-cooled dicing saw and have been exposed to atmospheric moisture for half a year.

V. Conclusion

It has been shown that by using an FHD-made overcladding with an appropriate thermal expansion coefficient, optical planar waveguides with very small birefringence can be made. Stresses in the core area resulting from the different thermal expansion of the substrate and the glass layer were calculated using finite element method. From the results we predict that the thermal expansion coefficient of the buffer and core glass, and the thickness of the substrate and the cladding do not influence the stress induced birefringence significantly. We have repeatedly overcladded cores of different compositions and in most instances have found low birefringence level. Some experiments indicated that the simplification used, namely the estimation of the birefringence just from an average of the refractive indices in the core region will not always work. Future work should address this by actually calculating the propagation constants for TE and TM-polarization resulting from the respective stress induced index modulation of the waveguide.

We are confident, that this is the most convenient method for removing the birefringence of the waveguides. No extra steps are required in the fabrication process. At the same time, no extra losses are produced, and we did not observe a deterioration of the filtering performance of the AWG's. Last, not least, we do not observe any problems with moisture sensitivity of the cladding glass, which had been an initially concern because of the high doping levels required.

Acknowledgment

The authors gratefully acknowledge E. Pawlowski's help in measuring the temperature dependent curvature of the wafer and E. Eberhardt for performing the lithography and etching of some of the samples.

References

[1] M. Kawachi, "Recent progress in silica-based planar lightwave circuits on silicon," *Inst. Elect. Eng. Proc.-Optoelectron.*, vol. 143, no. 5, pp. 257–262, 1996.
[2] Y. P. Li and C. H. Henry, "Silica-based optical integrated circuits," *Inst. Elect. Eng. Proc.-Optoelectron.*, vol. 143, no. 5, pp. 262–280, 1996.
[3] S. Suzuki *et al.*, "Polarization-insensitive arrayed-waveguide gratings using dopant-rich silica-based glass with thermal expansion adjusted to Si substrate," *Electron. Lett.*, vol. 33, no. 13, p. 1173, 1997.
[4] C. Henry, M. Milbrodt, and H. Yaffe, "Polarization compensated integrated optical filters and multiplexers," U.S. Patent 5 341 444.
[5] B. Green *et al.*, "Radiolytic modification of birefringence in silica planar waveguide structures," U.S. Patent 5 506 925.
[6] Y. Inoue *et al.*, "Polarization mde converter with polyimide half waveplate in silica based planar lightwave circuits," *IEEE Photon. Technol. Lett.*, vol. 6, no. 5, p. 626, 1994.
[7] M. Kawachi *et al.*, "Single mode channel optical waveguide with a stress-induced birefringence control region ," U.S. Patent 4 781 424.
[8] S. M. Ojha *et al.*, "Simple method of fabricating polarization insensitive and very low crosstalk AWG grating devices," *Electron. Lett.*, vol. 34, no. 1, p. 78, 1998.
[9] W. Vogel, *Glaschemie*, 3rd ed. Berlin, Germany: Springer, 1992.

[10] L. Maissel, "Thermal expansion of silicon," *J. Appl. Phys.*, vol. 31, p. 22, 1960.
[11] J. J. Wortman and R. A. Evans, "Young's modulus, shear modulus and Poisson's ratio in silicon and Germanium," *J. Appl. Phys.*, vol. 36, no. 1, p. 153, 1965.
[12] G. W. Scherer, "Stress-induced index profile distortions in optical waveguides," *Appl. Opt.*, vol. 19, no. 12, p. 2000, 1980.

A. Kilian, photograph and biography not available at the time of publication.

J. Kirchhof, photograph and biography not available at the time of publication.

B. Kuhlow, photograph and biography not available at the time of publication.

G. Przyrembel, photograph and biography not available at the time of publication.

W. Wischmann, photograph and biography not available at the time of publication.